Design Considerations for Supplemental Implants with Electrical Stimulation

By

Joshua Koski

Submitted to the graduate degree program in Mechanical engineering and the Graduate Faculty of the University of Kansas in partial fulfillment of the requirements for the degree of Master of Science.

_____
Chair: Dr. Elizabeth Friis

_____
Dr. Carl Luchies

_____
Dr. Sara Wilson

_____
Dr. Ifije Ohiorhenuan

Date Defended: December 3, 2020

The thesis committee for Joshua Koski certifies that this is the approved version of the following thesis:

Design Considerations for Supplemental Implants with Electrical Stimulation

_____

Chairperson: Dr. Elizabeth Friis

Date Approved: December 3, 2020

Abstract

After a severe fracture or damage to bone, many patients have a long road of recovery. In healthy patients, successful fusion can take 3 to 6 months, and even longer for high risk demographics. [1] Depending on the break most fractures are stabilized with fixation instrumentation such as, posterior rods, screws, or bone plates. This study looks into the application of pedicle screws and posterior rods for lumbar spinal fusion. To help decrease the risk of failure, surgeons will implement spinal fusion instrumentation to help provide increased stability as the bone heals. Instrumented spinal fusion has several advantages, such as no external immobilization, an early ambulation, along with improved rates of fusion. [2] Even with the advancements of medical devices lumbar fixation surgeries have a relatively high failure rate. It has been noticed that bone fusion can be benefited through electrical stimulation. Current electrical stimulation devices implement harmful batteries that need to be removed after they have run out of power. Piezoelectric material is a safe alternative power source that can be permanently implanted inside the body. Piezoelectric material has the capability to produce electric energy when stimulated through mechanical loading. Therefore, this study looks into the idea of utilizing piezoelectric ceramics to hone the mechanical loading produced in the body to generate beneficial electrical stimulation. Using finite element analysis (FEA), this study investigates the mechanical stresses transferred from the lumbar spine to fixation devices. With a better understanding of the stress distribution during everyday movements, we hope to use the compressive forces to promote healthy bone growth through electrical stimulation. The overall goal of this study is to show that, even with minimal force and low frequency applications, piezoelectric material can be strategically implemented onto already existing posterior rods and other orthopedic devices to promote faster and improved healing through clip-on devices.

Acknowledgements

Dr. Elizabeth Friis

I would like to thank Dr. Friis for providing me the opportunity to be a part of her lab. I am grateful to have the privilege to work under an advisor that is supportive and willing to guide me throughout my journey. As I finish up my time here at KU, I plan to carry on the values that Dr. Friis has passed on, we do research in hopes to help those in need and improve the lives of many.

Dr. Vijay Goel

I would like to thank Dr. Goel for his great insight and guidance in the field of spine biomechanics. I have learned a lot from Dr. Goel over our many virtual meetings over the past couple years.

Dr. Sara Wilson and Dr. Carl Luchies

I would like to thank Dr. Wilson and Dr. Luchies for serving on my committee. I really appreciated all the knowledge I have gained from their courses throughout my undergraduate and graduate journey here at KU.

Dr. Ifije Ohiorhenuan

I would like to thank Dr. Ohiorhenuan for serving on my committee and for his enthusiasm in this project in hope to see where this idea can go.

Amey Kelkar

I would like to thank Amey for all the help he has provided in the finite element analysis simulations necessary for this research project. Without Amey's involvement, this project would not have reached the level of success that it has.

My Lab mates at the University of Kansas

I would like to thank all my lab mates Ryan Downing, Ember Krech, Morgan Alters, Craig Cunningham, Tori Drapal, Jordan Gamble, Chris Tacca, Anna Norman, Evan Haas, and Luke

Lindemann for the knowledge you have shared with me to help me through the struggles of research. Getting to spend time with all of you really made research fun and I will always remember the time we made smores from a tiny stove in lab and all the other times that we sat around laughing, not getting work done.

Family

I would like to thank my family for always supporting me and pushing me to succeed no matter what the task. Without my family I would not be where I am today.

Table of Contents

Abstract iii
Acknowledgements iv
List of Figures viii
List of Tables viii
List of Equations viii
Chapter 1: Introduction 1
1.1 Background and Motivation 1
1.2 Specific aim 2
Chapter 2: Background and Literature Review 3
2.1 Bone healing 3
2.1.1 Failure of union 3
2.1.2 Electrical stimulation 4
2.2 Piezoelectricity 5
2.2.1 Piezoelectric material 6
2.2.2 Piezoelectric Applications 7
2.2.3 Piezoelectric effect for bone stimulation 8
2.3 Spinal fusion with posterior rods 9
2.3.1 Loading vertebrae with posterior fixation 10
2.4 Device Design 11
2.4.1 Intellirod Spine LOADPRO 11
2.4.2 Design History 11
2.5 Ultrasound 17
2.5.1 Ultrasounds Stimulation 17
2.6 References 18
Chapter 3: Journal of Medical Devices Research Paper 21
3.1 Abstract 22
3.2 Introduction 22
3.3 Methods and Materials 25
3.3.1 Rod Clip-On Device 25
3.3.2 Finite Element Model of Lumbar Spine 26
3.3.3 Material Properties 27
3.3.4 Loading and Boundary Conditions 28

3.4 Results 29
3.4.1 Compressive Loading 29
3.4.2 Physiological Bending 30
3.5 Discussion 31
3.6 Conclusion 34
3.8 References 34
Chapter 4: Conclusions and Future Work 37
4.1 Conclusion 37
4.2 Limitations 37
4.3 Future work 38
Appendix A: Detailed Methods 40
Appendix B: Other Stress Analysis 41
Appendix C: Rod Clip-on Device Electrode Location 43

List of Figures

Figure 1:Electric potentials produced by bone under mechanical loading 5
Figure 2: Piezoelectric effect of quarter ring stack 6
Figure 3: Poling Process for PZT a) before, b) during, c) after poling 7
Figure 4: Schematic of pedicle screws and posterior rods when a) no or low load is applied to the spine and b) when high load is applied to the spine 10
Figure 5: First Device Design a) Top view of device on posterior rod, b) posterior view of device on posterior rod, c) Isometric view of device and d) cross sectional isometric view of device 12
Figure 6: Second devise design a) Top view of device on posterior rod, b) posterior view of device on posterior rod, c) Isometric view of device and d) cross sectional isometric view of device 13
Figure 7: Testing apparatus used to find strain on posterior rod a) side view b) posterior view 13
Figure 8: Schematic of angles tested of the posterior rod with respect to the testing apparatus 14
Figure 9: Final device design a) Top view of device on posterior rod, b) posterior view of device on posterior rod, c) Isometric view of device and d) cross sectional isometric view of device 16
Figure 10: FEA device design a) Top view of device on posterior rod, b) posterior view of device on posterior rod, c) Isometric view of device and d) cross sectional isometric view of device 17
Figure 11: Final device design a) Top view of device on posterior rod, b) posterior view of device on posterior rod, c) Isometric view of device and d) cross sectional isometric view of device 25
Figure 12: L4-L5 Lumbar spine model a) Top view b) Posterior view C) Model without PLIF a PLIF cage and d) Model with a PLIF cage 27
Figure 13: Schematic plot of forces experienced by device attached to right posterior rod during walking. Adapted from Ref. [22] 33
Figure 14: ultrasound device design a) Top view of device on posterior rod, b) Posterior view of device on posterior rod, c) Isometric view of device and d) Cross sectional isometric view of device 39

List of Tables

Table 1: Posterior rod strain from posterior, 0 degrees, to anterior, 180 degrees, position 15
Table 2: Maximum compressive stress and respective force experienced by the rod clip-on device at the PZT stack location under compressive loading, in the Model without a PLIF cage 30
Table 3:Maximum compressive stress and respective force experienced by the rod clip-on device at the PZT stack location under compressive loading, in the Model with a PLIF cage 30
Table 4: Maximum respective compressive force experienced by the rod clip-on device at the PZT stack location under physiological bending, in the Model without a PLIF cage 31
Table 5: Maximum and respective compressive force experienced by the rod clip-on device at the PZT stack location under physiological bending, in the Model with a PLIF cage 31

List of Equations

Equation 1: Stress and equivalent force 29

Chapter 1: Introduction

1.1 Background and Motivation

On average, 6.8 million people break a bone each year in the United States, and it is estimated that every person will experience two bone breaks in their lifetime. Most will only encounter simple breaks where the bone only partially fractures and can be treated with simple immobilization like a splint or a cast. [3, 4] Those who experience more sever fractures, or full breaks in the bone will need to use fixation instrumentation to aid in the bone remodeling process. Even with the use of fixation systems the patient has a long road to recovery. Successful fusion can take 3 to 6 months and even longer for high risk demographics.

Fusion failure or nonunion is a very relevant issue when it comes to the remodeling of fractured or damaged bone. Bone is a complex tissue that relies on many mechanisms to successfully heal. Nonunion is common in patients who use tobacco, are diabetic, or have a high body mass index (BMI) as these factors negatively affect those necessary mechanism. [5, 6] Electrical stimulation has shown to help with these factors and benefit the bone healing process with one of the most advantageous therapies being direct current (DC) stimulation. DC electrical stimulation utilizes surgically implanted electrodes to apply an electric potential around the fusion site. [7]

Piezoelectric material has become popular in the field of electrical stimulation for bone healing. Current wireless medical devices require a power source, usually a battery which has a limited life span and must be replaced or removed. Piezoelectric material has been observed to be an alternative source for power generations. When a piezoelectric material experiences mechanical stress, it produces an electrical potential, defined as the piezoelectric effect. Studies have shown that piezoelectric material can be stimulated by physiological forces to generate

power for beneficial bone growth. It has also been identified that piezoelectric material can be stimulated by the mechanical energy produced from high frequency sound waves, a.k.a. ultrasound. This is beneficial for patients who cannot move for a long period of time after their operation. [8]

This study investigated the incorporation of piezoelectric material on preexisting medical devices, specifically, pedicle screw and posterior rod for lumbar fixation. A device was designed to contain a small quarter ring stack of PZT and clip onto a posterior rod between two pedicle screws. It was hypothesized that as the lumbar spine experienced mechanical loading, a compressive stress would be experienced by the PZT stack in the rod clip-on device. This PZT stack would then produce an electric potential in response to the mechanical stress, that would be utilized for DC electrical stimulation.

1.2 Specific aim

The main purpose of this study was to determine if piezoelectric material can be strategically implemented onto already existing orthopedic devices to promote fast and improved healing through a clip-on device for minimal force applications. This was accomplished by investigating the (1) stress distribution from the lumbar spine to a device clipped onto the posterior rod at various compressive loads and (2) observing if the occurring compressive force would be enough to generate power for electrical stimulation. It was hypothesized that, (1) during simulated walking the clip-on device would experience a compressive stress that originated from the lumbar spine and (2) the force experience by the piezoelectric stack would be great enough to generate power to be used in electrical stimulation.

Chapter 2: Background and Literature Review

2.1 Bone healing

Many factors play a role in bone healing and remodeling. This dynamic biological tissue is a structured rigid framework that utilized loads and many other biomechanical, cellular, hormonal, and pathological mechanisms to successfully fuse fractured or damaged bone. With all these factors in play, the success of spinal operations falls back on the restoration of the long-term spinal stability. [9] Implementing spinal instrumentation, such as posterior rods and pedicle screws, can benefit the stability of these operations in hopes of decreasing the risk of failure.

2.1.1 Failure of union

Fusion failure is the nonunion of the bone during the remodeling of a fracture. The Food and Drug Administration (FDA) classifies nonunion of a fracture after at least 9 months and has not shown signs of healing for 3 consecutive months. [10] In most cases it is better termed for when there are no signs of healing, increased pain or decrease in the functionally with respect to the procedure. Failure is a prevalent issue that surgeons and patients must deal with every year. The overall failure of lumbar spine surgery is estimated to be 10% to 46%, even with the advancement of spinal fusion procedures and devices, these rates have not changed as much as one would hope. After a failure, there is a need for a second and, or more necessary revision surgeries to fix the evolving issue. These follow up operations usually result in 70% failure rate for the second operations, 85% failure rate for the third and this trend continues. [11] Sadly this usually results in higher pain levels and can decrease the quality of life of the patient over time.

Many factors have been identified that cause an increase in the failure rate of bone remodeling. Studies have shown that it can take up to 3 to 6 months for fusion to occur, with posterior instrumentation implemented. [1] In that time there are a lot of things that could affect the success of fusion. Patient factors are one of the main reasons for spinal fusion failure today.

Patients that smoke are at greater risk of inhibiting spinal fusion and the risk of disc degeneration. In some cases, the quality of life decreases after surgery because of the bodies disability to promote bone growth. [5] It has also been observed that body mass index (BMI) can be used as a predictor for the outcome of spinal fusion operations. Patients with a higher BMI are at risk of experiencing postoperative complications, mainly infection. [6] The majority of surgeons will not operate on patients that are affected by these complications, knowing that there is an elevated risk of the procedure failing. Failure is not only determined by patient factors, there are many risks that come into play that fall back on the surgeon.

If the surgeon chooses to implement a spinal instrument into the procedure, they must make sure that their choice is appropriate for the specific application. Many patients have experienced poor outcomes due to inappropriate surgical choice, involving spinal instrumentation. [11]

2.1.2 Electrical stimulation

Electrical stimulation has been known to simplify the treatment of nonunion fractures for quite a while. It was identified in the early 1950's by Fukada et al. and Yasuda et al. that bone could transduce the mechanical loading it experienced into electric potentials. It was later in the 1950's that Shamos et al. and Lavine et al. characterized this as a piezoelectric effect. [12-14] It was demonstrated that bone was electronegative in areas of compression and this resulted in bone production. While bone was electropositive in areas of tension and this resulted in resorption of bone, shown in Figure 1.

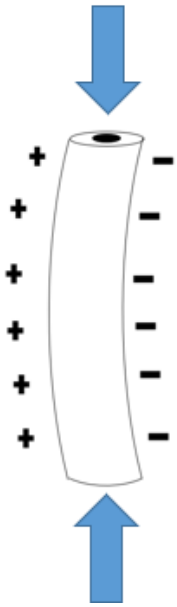

Figure 1:Electric potentials produced by bone under mechanical loading

It was then hypothesized that stimulating bone with these endogenous electric fields would result in advantageous bone healing. [15] There are three processes of administering electrical stimulation to bone which include direct current (DC), inductive coupling (IC) and capacitive coupling (CC). DC involves surgically implanting electrodes around the fracture site, with a power source providing the current. [7] IC utilized a pulsed electromagnetic field by placing coils around the fracture site over the skin. A current is sent through the coil which induces an electromagnetic field around the fracture site, enhancing the bone healing process. [16] Like IC, CC is a noninvasive process that involves placing electrodes on opposite sides of the fracture site, a power supply connected to the electrodes producing an electrical field around the fracture site. [17]

2.2 Piezoelectricity

Discovered in 1880 by Jacques and Pierre Curie, piezoelectricity is the ability of a material to produce an electric voltage that is proportional to the mechanical stress it is

experiencing, also known as the piezoelectric effect. This effect also allows the material to show proportional strain when a voltage is applied.

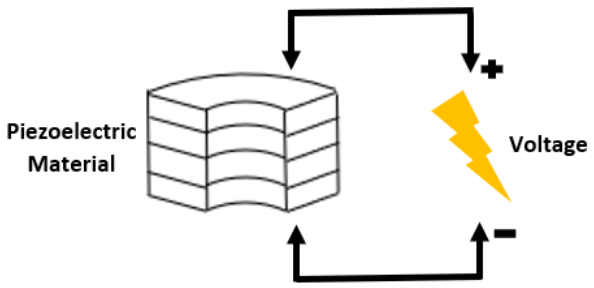

Figure 2: Piezoelectric effect of quarter ring stack

The developed charge is directly proportionate to the load that is being applied, as a compressive load generates a positive voltage, a tensile load will generate negative voltage. [18] When the material is experiencing stress that is influencing strain, there is an internal difference of charges that transpires, which entails the creation of a release of electrons that produce a voltage output. There are many materials that encompass piezoelectric properties, such as quartz, zinc oxide, lead-zirconate-titantae (PZT), barium titanate ($BaTiO_3$) and in this case bone. [19]

2.2.1 Piezoelectric material

Most piezoelectric material used in devices are mand-made, synthetic ceramics. For this study, lead-zirconate-titanate (PZT) rings and quarter rings are used to identify the effects of low volume on power outputs. PZT is a high-performance actuator and transducer ceramic that contains high dielectric and piezoelectric properties. PZT was chosen because of its inexpensive and strong attributes. [20] Synthetic materials are used more often because they can be altered to have greater piezoelectric effects, this is done via poling. Poling is achieved by introducing the piezoelectric ceramic to a strong electric field. This can be difficult depending on the ceramic shape. The direction of the electric field, or poling axis, determines the direction of the dipole

moments. The dipole moments arrange them self's in the same direction, then after the ceramic is removed from the electric field. The dipoles will shift slightly away from their poling position but remain in their new orientation permanently. [18] The direction of the dipole moments is the direction of the charge flowing through the ceramic during compression or the direction of strain when a voltage is applied.

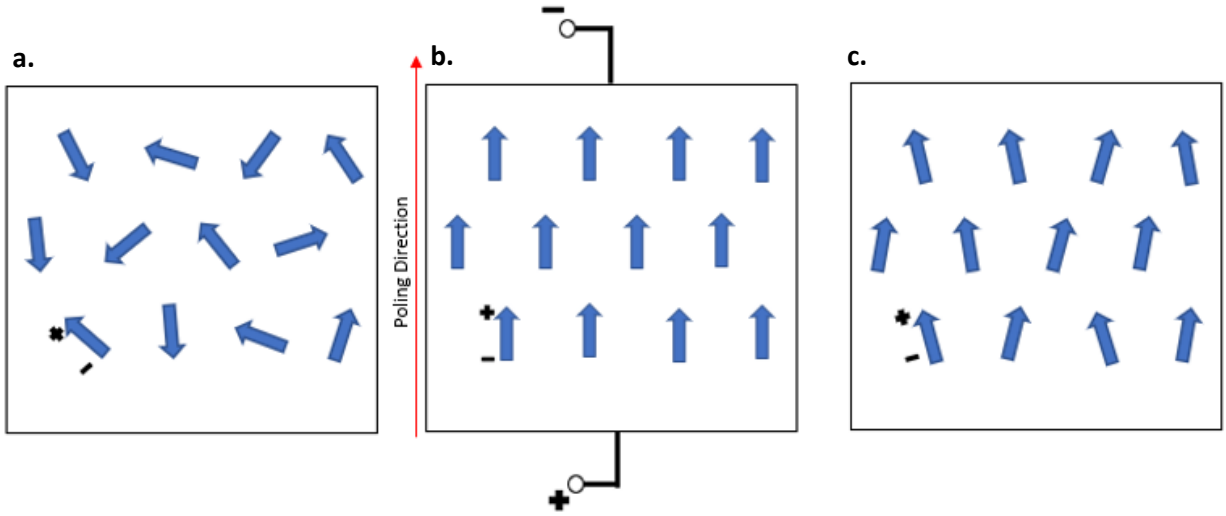

Figure 3: Poling Process for PZT a) before, b) during, c) after poling

As seen in Figure 3, after poling, the dipoles are oriented closer to their aligned position. This increases the piezoelectric property of the material by making it easier to align the dipoles when applying a force. Poling direction is important to this study, as it is looking into the potential power output of low volumes of PZT.

2.2.2 Piezoelectric Applications

Piezoelectric materials are used and designed for many applications such as displacement transducers, micro-positioners, rotary actuator, and sensors. [21] Different applications utilize piezoelectric properties in different ways. Actuators and micro-positioners take advantage of the electrical to mechanical properties of piezoelectric materials by applying an electric current to the piezoelectric to move and control a component of a system. Sensors benefits from the

mechanical to electrical properties of piezoelectric materials by using induced dynamic mechanical loading to output electrical signals. The greater the mechanical loading, the stronger the electrical voltage. Transducers can do both, they are used in small speakers and ultrasonic imaging because piezoelectric transducers have a high sensitivity and short-duration impulse responses. [22]

Piezoelectric materials have a variety of applicable functions. Medical devices that require wireless electronics are designed to utilize batteries as the power source. Batteries have the issue of having a limited lifespan and usually need another surgery to remove them, thus is why there is a need for a replacement. [23]

2.2.3 Piezoelectric effect for bone stimulation

The idea of using piezoelectric material in medical devices has been widely explored and is recently starting to be utilized to benefit tissue healing and bone remodeling. Piezoelectric ceramics can generate electrical signals under applied stress, which can stimulate the pathways of tissue regeneration at the damaged site. [24] While this is currently practiced through DC electrical stimulation, as mentioned before the battery has a limited lifespan and will need to be removed later down the line. With piezoelectric material producing power only when a mechanical load is applied, it can be permanently implanted. This concept has been tested in vivo and shows great potential. Friis et al. utilized direct current stimulation through piezoelectric composites in a vertebral interbody to identify spinal fusion rates in a pilot ovine study. Piezoelectric composites were stack and placed into an interbody cage, which was implanted near the fusion site of the ovine specimen. As the device experience mechanical loading, it delivered DC stimulation to the healing bone. [25] The results of this study show that

there is enough load to produce a healthy electrical signal to the fusion site and reemphasized electrical stimulation being a beneficial process of bone remodeling.

In low frequency applications, the total power generated is limited and struggles to be beneficial for electrical stimulation. These materials have been studied and further progressed to identify advanced parameters. Goetzinger et al. investigated the difference between a single layer and a variety of stacked layers of piezoelectric material (1 layer – 9 layers). It was observed that as the number of layers increased, the optimal load resistance decreased, making it more efficient to utilize piezoelectric material as a power source. [26] Krech et al. further investigated the effects of Compliant Layer Adaptive Composite Stacks (CLACS) implemented into piezoelectric stacks. Their findings show that CLACS have the ability to increase the efficiency of the power generated in low frequency applications while being able to keep the volume of piezoelectric material the same. [27]

2.3 Spinal fusion with posterior rods

Pedicle screws and posterior rods are one of the main spinal instruments that have been implemented into spinal surgery for many years. These stabilization instruments provide the advantage of decreasing the biomechanical stress on adjacent spinal segments and decrease the fatigue failure of other implants. [28] Studies have identified that the use of posterior instrumentation, has improved the patient's pain, mobility, rang of motion of spine, and the overall bone union. [29] Posterior rods are usually made from strong metals such as stainless steel, titanium, and chromium cobalt. Surgeons will bend the rods to better fit the contours of the patient's spine and fix them with the use of pedicle screws. Pedicle screws are placed at the junction of the lateral facet and the transverse processes of the lumbar spine. [30] Studies have identified that pedicles are at risk of loosening, breaking, bending, and sometimes reducing the

mobility of the spine. [31] In some cases, posterior rods are made from polyether ether ketone (PEEK). Surgeons may utilize this material to implant dynamic posterior fixation, as the PEEK is a more flexible material, and this allows the patient to have more mobility post operation. PEEK rods do not offer the same amount of stability for the spine and should be used in specific spinal fixation applications.

2.3.1 Loading vertebrae with posterior fixation

With posterior rods and pedicles screws implanted into the body, they take some of the biomechanical loads off the spine and the load is distributed differently across the vertebral disk. With the posterior position of the vertebrae being fixed by the posterior rod, under high loads it is unable to compress with the rest of the vertebrae during axial loading, seen in Figure 4

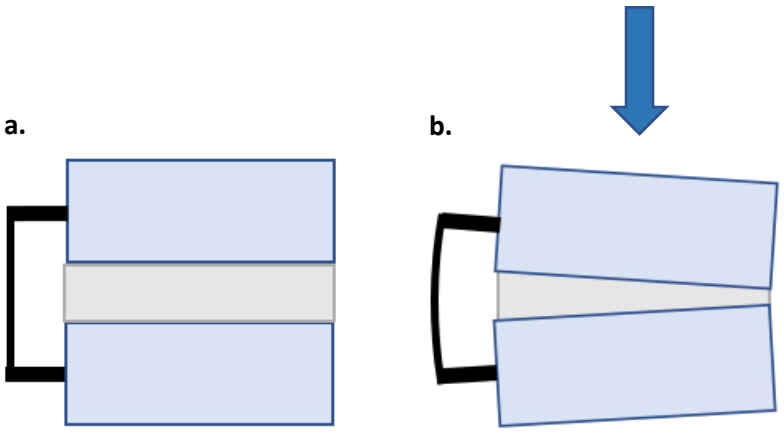

Figure 4: Schematic of pedicle screws and posterior rods when a) no or low load is applied to the spine and b) when high load is applied to the spine

With a simple 4 pedicle screw, bilateral posterior rod set up across two vertebrae, it was noticed that posterior rods are able to distribute 43% of the load away from the vertebral column. [32] As the posterior fixation spans across more vertebrae, utilizing more pedicle screws and longer posterior rods, the load distribution can increase, and more stress can be taken off the vertebral column. Less stress on the spine during union minimizes the risks of failure.

Understanding the load distribution from the vertebrae to the posterior rod is important to this study.

2.4 Device Design

As the rod clip-on device was being designed it went through many iterations to meet the criteria of surgeons and FDA predicate devices.

2.4.1 Intellirod Spine LOADPRO

Intellirod Spine LOADPRO is a spinal implant used to monitor the strain experienced on a posterior rod, during operation. The LOADPRO is implanted between two pedicle screws and sends data via wireless radio-frequency-identification (RIFD) sensors. The main goal of this device is to help surgeons quantify the tactile feel of the forces that are being applied during deformity correction surgery. In 2019 the LOADPRO was approved for De Novo by the FDA to clamp on to 5.5mm rods for the use of analyzing rod strain during kyphotic correction surgery. With the data obtained from the LOADPRO surgeons are able to gain a better understanding of the strain levels that correlated to the yield limits of the rod material. [33, 34]

2.4.2 Design History

The design of the LOADPRO was used as a predicate design for the rod clip-on device of this study. After reaching out to surgeons, specifications were made to develop an initial prototype. Surgeons noted that there is very little posterior space between lumbar vertebrae, especially after implanting a fixation instrumentation. It was noted that the bulk of the device should be either posterior to the rod or lateral to the rod, to ensure that the rod clip-on device will not interfere with spinal mobility. With these specification in hand, and a preliminary design from the LOADPRO, an initial design was developed, shown in Figure 5

The rod clip-on device had a compartment for the piezoelectric stack and a circuit, the device attached to the rod from the medial. Screws would then be used to tighten the device onto

the rod. Further through customer discovery, surgeons prefer to have the piezoelectric stack and circuit, bulk of the device, to be place lateral to the rod. This will allow the surgeon to have room to place bone graft, and to minimize the risk of the rod clip-on device interfering with the lumbar spine. The design of the rod clip-on device was changed to fit this criterion. (Figure 5)

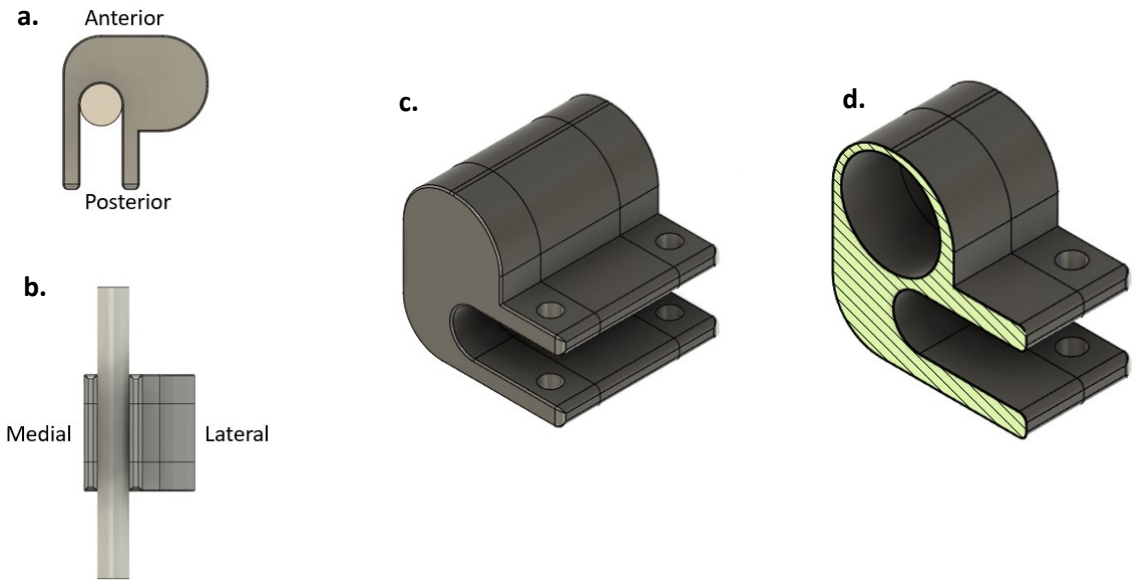

Figure 5: First Device Design a) Top view of device on posterior rod, b) posterior view of device on posterior rod, c) Isometric view of device and d) cross sectional isometric view of device

By rotating the rod clip-on device, it was then noticed that the surgeon will need to tighten the screws from the lateral side of the rod, which would be very difficult with how little room the surgeon must work with during the lumbar fusion procedure. To address this issue, the design of the tulip of a pedicle screw was used as inspiration. The device would then attach to the rod from the anterior, and a set screw would be placed and tightened from the posterior. Surgeons noted that there is 8 mm to 10 mm between pedicle screws on adjacent vertebrae in most applications. The overall top to bottom thickness of the rod clip-on device needed to be adjusted to mee this new criteria.

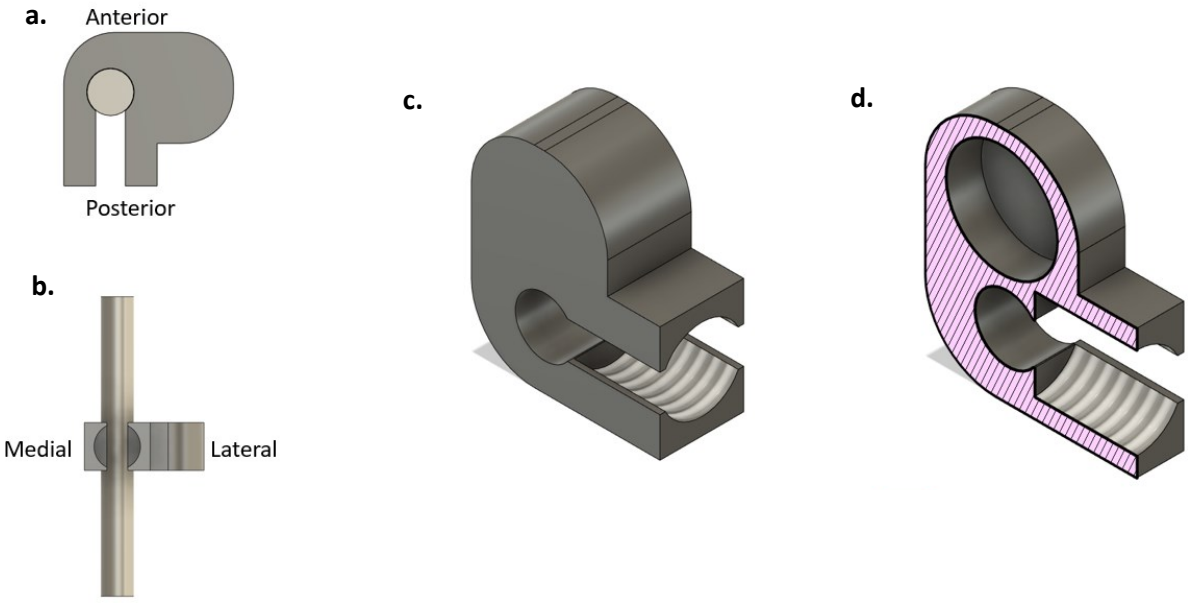

Figure 6: Second devise design a) Top view of device on posterior rod, b) posterior view of device on posterior rod, c) Isometric view of device and d) cross sectional isometric view of device

Device in Figure 6 has a top to bottom thickness of 8mm. Minimizing the overall thickness of the rod clip-on device, makes it easier to place between adjacent pedicle screws, but minimizes the amount of piezoelectric material able to be place inside.

To determine the best location for the PZT in the rod clip-on device with respect to the posterior fixation instrumentation, a testing apparatus (Figure 7) was compressed in a uniaxial MTS. A strain gauge was attached to the center of the posterior rod, where the rod clip-on device would be located, and the rod was placed into the testing setup.

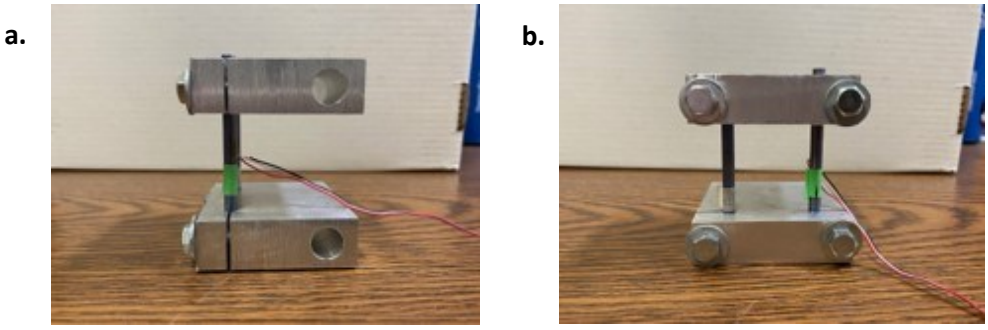

Figure 7: Testing apparatus used to find strain on posterior rod a) side view b) posterior view

With the stain gauge located in the posterior most position of the rod, with respect to the setup, a compressive force of 0 N, 100 N, 200 N, 300 N, 400 N and 500 N was applied to the testing apparatus. The rod was rotated laterally 0º, 15º, 30º, 45º, 60º, 75º, 90º, 105º, 120º, 135º, 150º, 165º and 180º until the strain gauge was located in the anterior most position, with respect to the testing setup (Figure 8). Same compressive loads were applied at each angle. This was done to identify at what point the rod will experience the greatest maximum compressive stress.

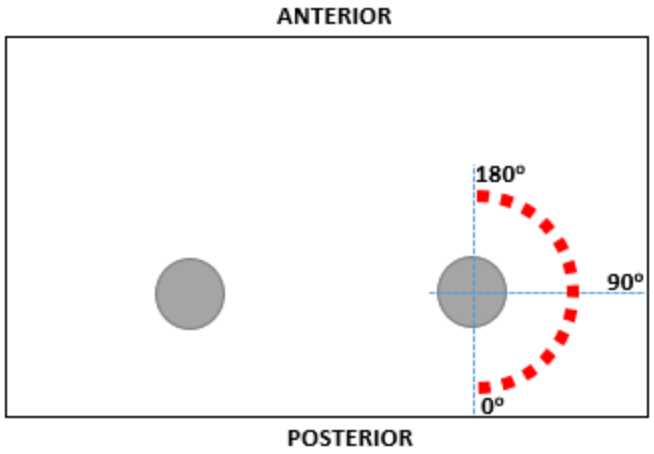

Figure 8: Schematic of angles tested of the posterior rod with respect to the testing apparatus

Strain (με) was recorded at each angle for various compressive loads. Seen in table 1, as the strain gauge was rotated from its posterior most position, 0º, to its anterior most position, 180º, the strain experienced changes from positive to negative. This shows that the rod is experiencing tensile forces on its posterior side and compressive forces on its anterior side. As the angle increased the strain drops, and as the angle approached 90º the strain approached 0με, meaning the neutral axis is located near 90º. Minimal strain should be experienced around 90º as the neutral axis does will not experience tensile nor compressive strain. For all load conditions this trend is consistent. As the compressive force is increased from 0 N to 500 N, the experienced

strain is also increased positively on the posterior side, 0º, and negatively on the anterior side, 180º.

Table 1: Posterior rod strain from posterior, 0 degrees, to anterior, 180 degrees, position

Force (N)	*Strain at 0 Degrees (με)*	*Strain at 15 Degrees (με)*	*Strain at 30 Degrees (με)*	*Strain at 45 Degrees (με)*	*Strain at 60 Degrees (με)*	*Strain at 75 Degrees (με)*	*Strain at 90 Degrees (με)*	*Strain at 105 Degrees (με)*	*Strain at 120 Degrees (με)*	*Strain at 135 Degrees (με)*	*Strain at 150 Degrees (με)*	*Strain at 165 Degrees (με)*	*Strain at 180 Degrees (με)*
0	0	0	0	0	0	0	0	0	0	0	0	0	0
100	1033	952	866	688	454	50	-203	-460	-670	-879	-896	-1017	-1066
200	2042	1866	1701	1327	840	116	-398	-913	-1299	-1708	-1758	-2023	-2098
300	3066	2800	2474	1952	1262	143	-621	-1367	-1930	-2510	-2647	-3055	-3112
400	4110	3726	3271	2572	1651	179	-842	-1834	-2576	-3397	-3575	-4060	-4144
500	5224	4684	4085	3208	2058	206	-1063	-2301	-3218	-4239	-4517	-5100	-5161

PZT material performs best in compressive loading environments. This test was implemented to identify the best location to place the PZT material in the rod clip-on device, in reference to the posterior fixation instrumentation. Looking at table 1. strain distribution around the posterior rod translates from tensile to compressive as the strain gauge was rotated from 0º to 180º. The neutral axis is located near 90º as the strain decreases when the strain gauge was approaching that angle. With the anterior position of the rod experiencing the maximum compressive strain, it was decided that the design of the rod clip-on device would place the PZT material in that location.

It was analyzed that the maximum stress would be experienced on the anterior side of the rod. The final iteration of the rod clip-on device places the piezoelectric stack in the anterior position, and the device is adhered to the rod through a set screw on the posterior. There is very little space between the posterior rod and the vertebrae anterior to it. The rod clip-on device design has a compartment for quarter rings of piezoelectric material, that wrap around the curvature of the rod and allows the stack to be very close to the rod itself. As the rod is bent anteriorly, during everyday movement, the stack can be compressed. The choice to place the

piezoelectric stack so close to the rod, is to increase the transferred force from the rod to the device, and to make sure that the rod clip-on device would not interfere with the lumbar spine.

The rod clip-on device for this study was designed to clip on to a 5.5mm posterior rod. The device was attached the same way that a pedicle screw attaches to a rod, there was an insert for the rod and a setscrew was used to tighten the device to the rod. A piezoelectric stack was placed in the rod clip-on device, which was utilized for power generations through compressive loading.

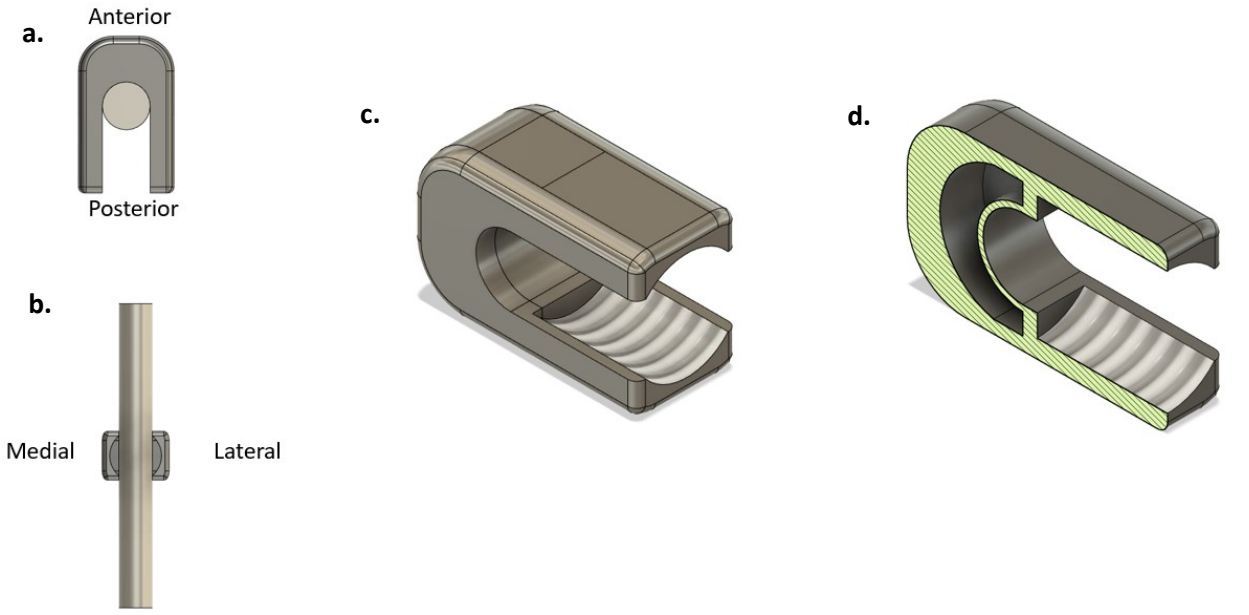

Figure 9: Final device design a) Top view of device on posterior rod, b) posterior view of device on posterior rod, c) Isometric view of device and d) cross sectional isometric view of device

Finite element analysis (FEA) was used to run the simulations in this study. The rod clip-on device was attached onto a posterior rod modeled in Abaqus FE solver. To ensure that the device is completely fixed to the posterior rod, the rod clip-on device design was simplified. The location of the set screw on the rod clip-on device was filled in to allow the device to be fixed completely around the posterior rod.

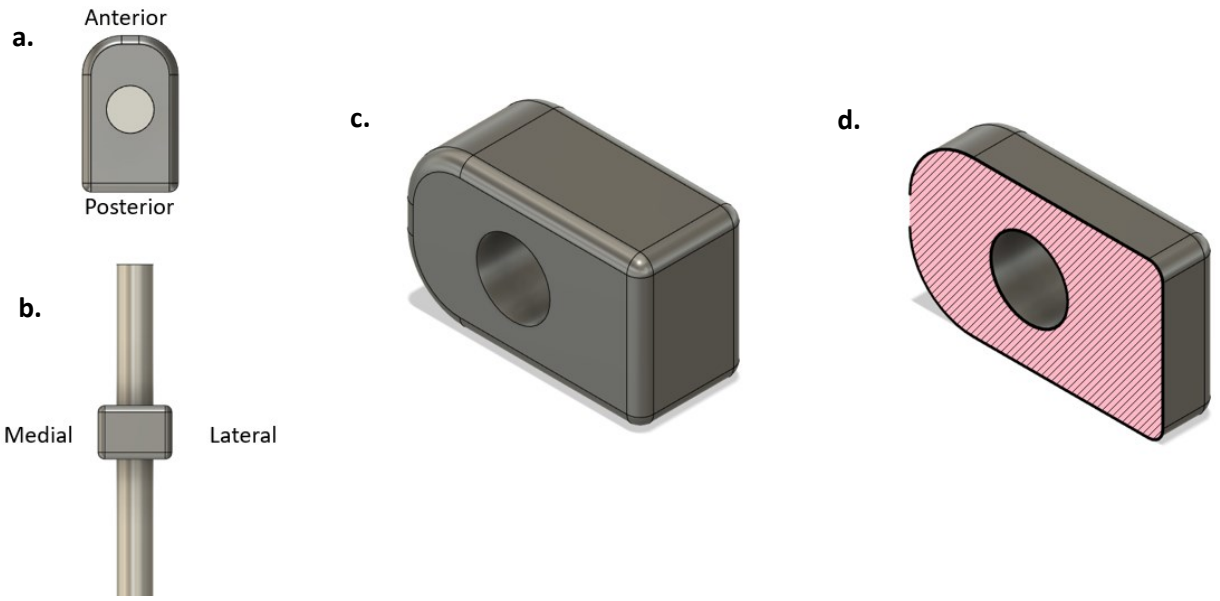

Figure 10: FEA device design a) Top view of device on posterior rod, b) posterior view of device on posterior rod, c) Isometric view of device and d) cross sectional isometric view of device

2.5 Ultrasound

Ultrasound is a wave signal that transports mechanical energy through vibration of the medium it travels through, to be classified as ultrasound the signal much operate at frequencies of 20 kHz or higher, with no net transport of the particles of the medium themselves. [35] Ultrasounds has been used as early as 1940's for sonar and radar technology and soon thereafter was developed and adapted in the 1950's for diagnostic imaging for cancerous tissue. [36] In the medical field, ultrasound is widely used for diagnosis and therapeutic treatment. This study will look into the mechanical energy produced through ultrasound to stimulate the mechanical to electrical properties of piezoelectric materials for electrical stimulation.

2.5.1 Ultrasounds Stimulation

Therapeutic ultrasound has been used for many years. Early adaptations utilized ultrasound for tissue heating. It was soon seen to benefit in stimulating the physiological healing process for tissue repair at low intensity levels and used for controlled tissue ablation at high intensity levels. [37] It was recently studied that ultrasound could be used to stimulate

piezoelectric material and generate power. Alters et al. investigated the efficacy of using ultrasound to stimulate piezoelectric material for power generation. This study tested stacked piezoelectric material, along with CLACS integration. It was observed that stimulating the material parallel to that of its poling direction can generate power. With the involvement of CLACS this power was increased. [8]

2.6 References

1. Nam, W. D., and Yi, J., 2016, "Bone Union Rate Following Instrumented Posterolateral Lumbar Fusion: Comparison between Demineralized Bone Matrix versus Hydroxyapatite," Asian Spine J, **10**(6), pp. 1149–1156.
2. Soo Suk, K., Mo Lee, H., Hyun Kim, N., and Won Ha, J., 2000, "Unilateral Versus Bilateral Pedicle Screw Fixation in Lumbar Spinal Fusion," Spine, **25**(14), pp. 1843–1847.
3. "Fracture - Mediniche, Inc." [Online]. Available: https://www.mediniche.com/fracture.html. [Accessed: 15-Nov-2020].
4. "Arm Injury Statistics | Aids for One Armed Tasks" [Online]. Available: https://u.osu.edu/productdesigngroup3/sample-page/. [Accessed: 15-Nov-2020].
5. Sandén, B., Försth, P., and Michaëlsson, K., 2011, "Smokers Show Less Improvement than Nonsmokers Two Years after Surgery for Lumbar Spinal Stenosis: A Study of 4555 Patients from the Swedish Spine Register," Spine, **36**(13), pp. 1059–1064.
6. Jackson, K. L., and Devine, J. G., 2016, "The Effects of Obesity on Spine Surgery: A Systematic Review of the Literature," Global Spine J, **6**(4), pp. 394–400.
7. Griffin, M., and Bayat, A., 2011, "Electrical Stimulation in Bone Healing: Critical Analysis by Evaluating Levels of Evidence," Eplasty, **11**.
8. Alters, M., 2019, "Determination of Clinical Efficacy of Ultrasound Stimulation on Piezoelectric Composites for Power Generation Applications," M.S., University of Kansas.
9. Kalfas, I. H., 2001, "Principles of Bone Healing," Neurosurgical Focus, **10**(4), pp. 1–4.
10. Calori, G. M., Mazza, E. L., Mazzola, S., Colombo, A., Giardina, F., Romanò, F., and Colombo, M., 2017, "Non-Unions," Clin Cases Miner Bone Metab, **14**(2), pp. 186–188.
11. Daniell, J. R., and Osti, O. L., 2018, "Failed Back Surgery Syndrome: A Review Article," Asian Spine J, **12**(2), pp. 372–379.
12. Yasuda, I., *Piezoelectricity of Living Bone.* Journal of Kyoto Prefectural University of Medicine, 1953. **53**(325).
13. Fukada, E. and I. Yasuda, *On the Piezoelectric Effect of Bone.* Journal of the Physical Society of Japan, 1957. **12**(10): p. 5.
14. Lavine, L. S., and Grodzinsky, A. J., 1987, "Electrical Stimulation of Repair of Bone.," JBJS, **69**(4), pp. 626–630.
15. Black, J., 1986, "Electrical Stimulation: Its Role in Growth, Repair and Remodeling of the Musculoskeletal System."
16. Evans, R. D., Foltz, D., and Foltz, K., 2001, "Electrical Stimulation with Bone and Wound Healing," Clinics in Podiatric Medicine and Surgery, **18**(1), pp. 79–95, vi.

17. Kooistra, B. W., Jain, A., and Hanson, B. P., 2009, "Electrical Stimulation: Nonunions," Indian J Orthop, **43**(2), pp. 149–155.
18. Jaffe, B., 2012, *Piezoelectric Ceramics*, Elsevier.
19. Guerin, S., Tofail, S. A. M., and Thompson, D., 2019, "Organic Piezoelectric Materials: Milestones and Potential," NPG Asia Materials, **11**(1), pp. 1–5.
20. Zhang, S., Xia, R., and Shrout, T. R., 2006, "Lead-Free Piezoelectric Ceramics vs. PZT?," *2006 15th Ieee International Symposium on the Applications of Ferroelectrics*, pp. 201–207.
21. Wu, C. C. M., Kahn, M., and Moy, W., 1996, "Piezoelectric Ceramics with Functional Gradients: A New Application in Material Design," Journal of the American Ceramic Society, **79**(3), pp. 809–812.
22. San Emeterio, J. L., and Ramos, A., 2004, "Models for Piezoelectric Transducers Used in Broadband Ultrasonic Applications," *Piezoelectric Transducers and Applications*, A. Arnau Vives, ed., Springer, Berlin, Heidelberg, pp. 55–67.
23. Anton, S. R., and Sodano, H. A., 2007, "A Review of Power Harvesting Using Piezoelectric Materials (2003–2006)," Smart Mater. Struct., **16**(3), p. R1.
24. Jacob, J., More, N., Kalia, K., and Kapusetti, G., 2018, "Piezoelectric Smart Biomaterials for Bone and Cartilage Tissue Engineering," Inflamm Regener, **38**(1), p. 2.
25. Friis, E.A., S.N. Galvis, and P.M. Arnold, *DC Stimulation for Spinal Fusion with a Piezoelectric Composite Material Interbody Implant: An Ovine Pilot Study*. 2015.
26. Goetzinger, N.C., et al., *Composite piezoelectric spinal fusion implant: Effects of stacked generators.* J Biomed Mater Res B Appl Biomater, 2016. **104**(1): p. 158-64.
27. Krech, E.D., et al., *Effect of compliant layers within piezoelectric composites on power generation providing electrical stimulation in low frequency applications.* J Mech Behav Biomed Mater, 2018. **88**: p. 340-345.
28. Tyagi, V., Strom, R., Tanweer, O., and Frempong-Boadu, A. K., 2018, "Posterior Dynamic Stabilization of the Lumbar Spine Review of Biomechanical and Clinical Studies," Bulletin of the Hospital for Joint Disease (2013), **76**(2), pp. 100–104.
29. Khan, K. M., Bhatti, A., and Khan, M. A., 2012, "Posterior Spinal Fixation with Pedicle Screws and Rods System in Thoracolumbar Spinal Fractures," Journal of the College of Physicians and Surgeons--Pakistan: JCPSP, **22**(12), pp. 778–782.
30. "Pedicle Screw Placement" [Online]. Available: https://www.medschool.lsuhsc.edu/neurosurgery/nervecenter/tlscrew.html. [Accessed: 07-Oct-2020].
31. Katonis, P., Christoforakis, J., Aligizakis, A. C., Papadopoulos, C., Sapkas, G., and Hadjipavlou, A., 2003, "Complications and Problems Related to Pedicle Screw Fixation of the Spine," Clinical Orthopaedics and Related Research®, **411**, pp. 86–94.
32. Gioia, G., Scotti, C., Mandelli, D., and Sala, G., 2011, "Posterior Spinal Instrumentation: Biomechanical Study on the Role of Rods on Hardware Response to Axial Load," Eur Spine J, **20**(Suppl 1), pp. 3–7.
33. 2019, "Intellirod Spine Receives First-Ever Spine FDA De Novo Approval" [Online]. Available: https://www.businesswire.com/news/home/20190401005572/en/Intellirod-Spine-Receives-First-Ever-Spine-FDA-De-Novo-Approval. [Accessed: 09-Oct-2020].
34. "Intellirod Spine™ (Formerly OrthoData Inc.) | LOADPRO™ Intraoperative Rod Strain Sensor" [Online]. Available: http://www.intellirodspine.com/LOADPRO.html. [Accessed: 19-Nov-2020].

35. Leighton, T. G., 2007, “What Is Ultrasound?,” Progress in Biophysics and Molecular Biology, **93**(1), pp. 3–83.
36. Shung, K. K., 2015, *Diagnostic Ultrasound: Imaging and Blood Flow Measurements, Second Edition*, CRC Press.
37. ter Haar, G., 1999, “Therapeutic Ultrasound,” European Journal of Ultrasound, **9**(1), pp. 3–9.

Chapter 3: Journal of Medical Devices Research Paper

This section contains a manuscript to be submitted for publication with The Journal of Medical Devices

Design Considerations for Supplemental Implants with Electrical Stimulation

Authors:

Joshua Koski
Spine Biomechanics Laboratory,
Department of Mechanical,
University of Kansas,
Lawrence, KS, 66045
Email: jkosk@ku.edu

Ryan Downing
Spine Biomechanics Laboratory,
Department of Bioengineering,
University of Kansas,
Lawrence, KS, 66045
Email: ryandowning@ku.edu

Amey Kelkar
Research and Develop Engineer,
Department of Bioengineering,
University of Toledo,
Toledo, OH 43606
Email: amey.kelkar@utoledo.edu

Ifije Ohiorhenuan
Assistant Professor,
Department of Neurosurgery,
University of Kansas Medical Center,
Kansas City, KS 66160
Email: iohiorhenuan@kumc.edu

Elizabeth Friis
Professor,
Department of Mechanical Engineering,
University of Kansas,
Lawrence, KS 66045
Email: lfriis@ku.edu

Vijay Goel
Professor,
Departments of Bioengineering and Orthopaedical Surgery,
University of Toledo,
Toledo, OH 43606
Email: Vijay.goel@utoledo.edu

3.1 Abstract

After a spinal fusion, many patients have a long road to recovery. In healthy patients, spinal fusion can take three to six months, and even longer for high risk populations. The majority of spinal fusions are stabilized with fixation implants, posterior rods, screws, or bone plates. These devices are minimally invasive and quick to implant, yet the rate of recovery is still a growing issue. It has been discovered that the rate of bone fusion can be increased through electrical stimulation. Thus, recovery rates can be increased to get patients back to their everyday lives faster. A safe way to implement a power source inside the body is with the use of piezoelectric materials, a material that produces electric energy when stimulated via mechanical loading. By utilizing piezoelectric ceramics, we can hone the mechanical loading from everyday movement to produce beneficial electric stimulation. The main scope of this study is focused on spinal fusion. By identifying the load transfer and stress distribution from the spine to fixation devices, via finite element analysis and mechanical testing, we hope to understand and utilize the compressive forces to promote healthy bone growth through electrical stimulation. The overall goal of this study is to show that, even with minimal force applications, piezoelectric materials can be strategically implemented onto already existing posterior rods and other orthopedic devices to promote faster and improved healing through clip-on devices.

3.2 Introduction

It is estimated that every year in the united states, approximately 6.8 million people break a bone. It is also estimated that every person will break at least two bones in their lifetime. [1,2] Bone being a dynamic biological tissue, it relies on many biomechanical, cellular, hormonal, and pathological mechanisms to successfully heal fractured or damaged bone. [3] To aid in beneficial bone remodeling, fixation instrumentation is usually implemented into the procedure to help increase the stability of the fusion site and decrease the possible risk of failure.

If the damaged bone does not show signs of healing, if there is an increase in pain or decrease in functionality then there is most likely a result of nonunion. The overall failure of lumbar spinal operations is estimated to be 10% to 46%, even with the current advancements in procedures and medical devices. This leads to revision surgery and results in an increased chance of the operation failing one again. [4] With failure rates being so high, surgeons are cautious to operate on demographics such as tobacco users, patients with a high body mass index (BMI) and elderly patients due to their lowered ability to promote bone growth and their history of postoperative complications. [5, 6]

Electrical stimulation has been known to simplify the treatment of nonunion fractures for quite a while. In the 1950's it was identified that bone produced electrical potentials when it experienced mechanical loading, this was characterized as a piezoelectric effect. [7-9] It was observed that bone was electronegative in areas of compression and electropositive in areas of tension, this resulted in beneficial bone production and resorption, respectively. It was later hypothesized that placing damaged bone into an electric field would result in advantageous bone healing. [10] The most common electrical stimulation therapies used to benefit bone remodeling are direct current (DC), inductive coupling (IC) and capacitive coupling (CC). This study will focus on the DC electrical stimulation. DC involves implanting electrodes around the fracture site and using a power source to supply an electric current to the electrodes. [11]

Current wireless electrical stimulation devices utilize batteries as their power source, the issue with this comes later down the line when the battery has reached the end if its lifespan and must be surgically removed. With piezoelectric material, the device can be permanently implanted. [12] Piezoelectric materials have the ability to produce an electric potential that is proportional to the mechanical stress that it experiences, and vice versa. There are many

materials that encompass piezoelectric properties such as quartz, zinc oxide, lead-zirconate-titanate (PZT), barium titanate ($BaTiO_3$) and in this case bone. [13] The main focus of this study incorporates the properties of a PZT stacks being stimulates by physiological forces in the body.

Piezoelectric material in medical devices has been widely explored and is recently being utilized to benefit tissue healing and bone remodeling via DC electrical stimulation. Friis et al, implemented a PZT stack into an interbody cage and showed that the PZT stack experienced mechanical loading from physiological forces in an ovine study. The mechanical loading experienced was used for DC stimulation to help fuse the bone at that site. [14] PZT stack configurations were further studied by Goetzinger et al. who discovered that increasing the number of PZT layers in a stack helps lower the optimal load resistance, making the PZT a more efficient power source. [15] Krech et el. discovered that implementing Compliant Layer Adaptive Composite Stacks (CLACS) increases the efficiency of the power generation in low frequency applications with a low volume of PZT material. [16]

This study investigated the incorporation of piezoelectric material on preexisting medical devices, specifically, pedicle screw and posterior rod for lumbar fixation. A device was designed to contain a small quarter ring stack of PZT and clip onto a posterior rod between two pedicle screws. Cunningham et al. investigated the behavior of 15 mm outer-diameter x 8.5 mm inner-diameter x 0.7 mm thick PZT ring stack under compressive loading. [17] Due to the limited space in the rod clip-on device, this study analyzes quarter rings of the PZT rings used in that study. It was hypothesized that as the lumbar spine experienced mechanical loading, a compressive stress would be experienced by the PZT stack in the rod clip-on device. This PZT stack would then produce an electric potential in response to the mechanical stress, that would be utilized for DC electrical stimulation.

3.3 Methods and Materials

3.3.1 Rod Clip-On Device

Parts were designed, through Autodesk's Fusion 360 and SolidWorks computer aided design (CAD) programs. CAD offered quick and accurate prototyping along with simulation software which was used to gain preliminary data for finite element analysis (FEA). Rod clip-on device was designed to the specifications obtained through customer discovery. After talking with surgeons and professionals in the field of spinal fusion, many design iterations were made to meet the needs of both the surgeon and the mechanical properties of the PZT material incorporated in the device. The final iteration of the design mimics the design and functionality to that of the tulip of a pedicle screw. The rod clip-on device will be implanted between two pedicle screws on to the posterior rod and will be held in place with a set screw. The rod clip-on device is threaded to allow a set screw to be used to tighten the connection between the rod and the device. A compartment that contains the PZT stack is located anterior to the rod.

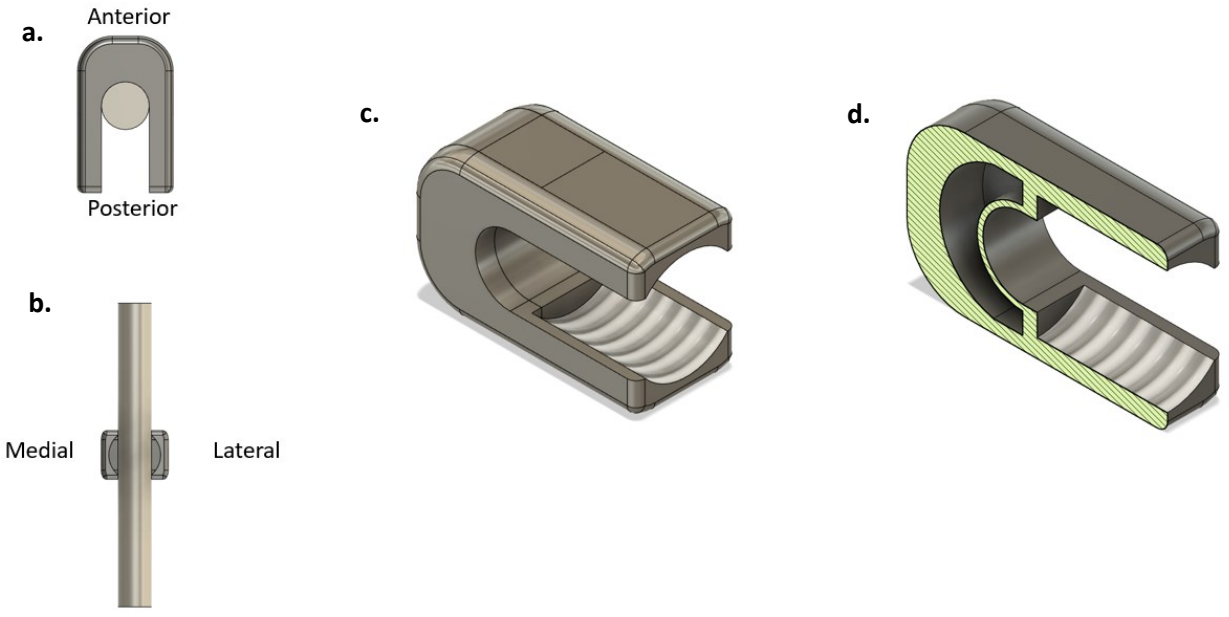

Figure 11: Final device design a) Top view of device on posterior rod, b) posterior view of device on posterior rod, c) Isometric view of device and d) cross sectional isometric view of device

3.3.2 Finite Element Model of Lumbar Spine

A L4-L5 lumbar spine finite element model was used for this study. The model was derived from a T1-S1 computer tomography (CT) scan of a healthy adult subject and transferred into ABAQUS FE solver. Developed at the university of Toledo, the model has been validated through well documented studies and has been widely utilized for analyzing clinically relevant issues. [18-24**]** Vertebral bodies were modeled with a thick cortical bone shell surrounding a cancellous porous bone core. Intervertebral disc consisted of a solid ground substance that is reinforced with embedded fibers. Ligaments were modelled as truss elements and facet joints were derived using three-dimensional gap elements. (Figure 11) FEA simulations were simulated on two L4-L5 lumbar models. The first model, Model without a PLIF cage, consisted of the L4-L5 lumbar implanted with four 6.5 mm diameter x 45 mm in length pedicle screws and two 5.5 mm diameter posterior rods. The second model, Model with a PLIF cage, consisted of the L4-L5 lumbar implanted with the same pedicle screw and rod instrumentation, along with a posterior lumbar interbody fusion (PLIF) cage placed in between the L4-L5 disc space replacing the intervertebral disc. The rod clip-on device was imported into both models and was fixed to the center of the right posterior rod.

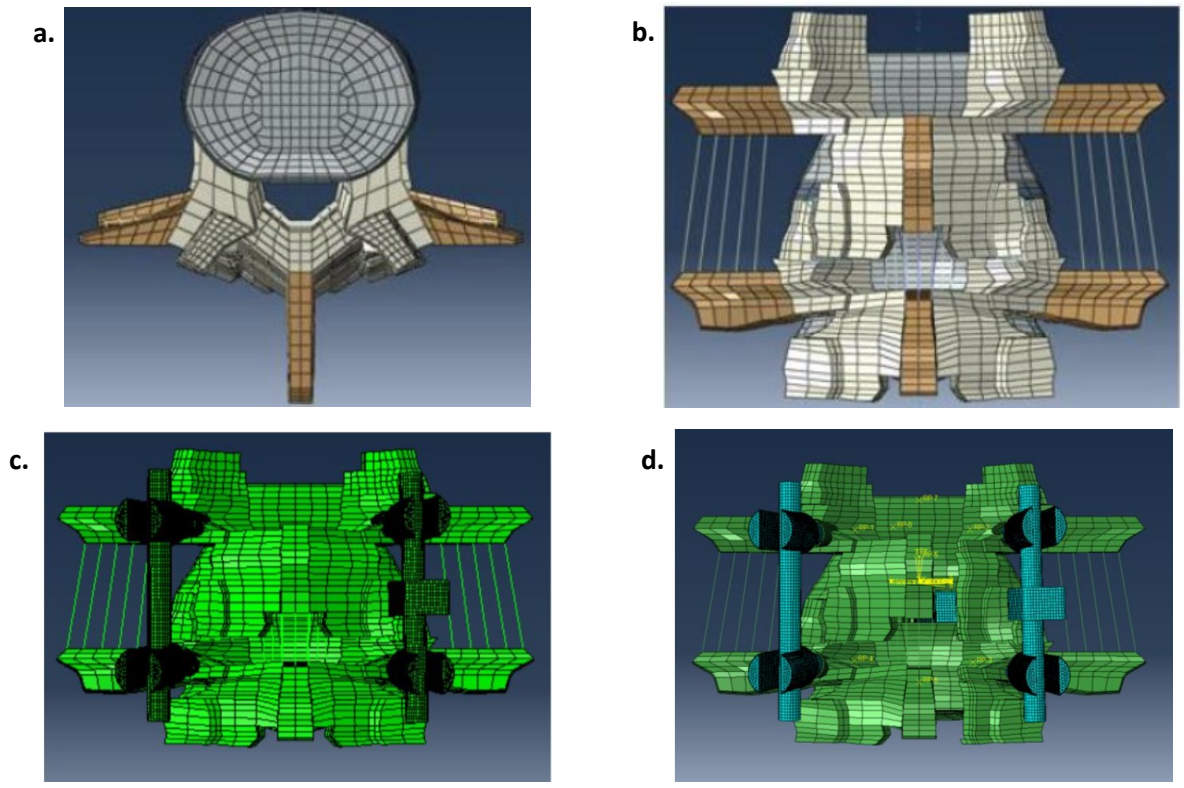

Figure 12: L4-L5 Lumbar spine model a) Top view b) Posterior view C) Model without PLIF a PLIF cage and d) Model with a PLIF cage

3.3.3 Material Properties

The material properties remained constant between both L4-L5 lumbar spine models tested in this study. Cortical bone, cancellous bone, nucleus pulposus, and annulus solid ground were modeled with hexahedral elements, and the annulus fibers were modeled with rebar elements. Ligaments were modeled as truss elements and facet joints were derived using three-dimensional gap elements. (Figure 11) Posterior fixation instruments were modeled with hexahedral elements and linear elastic behavior was assumed. Pedicle screws and rods were simulated with Ti6AI4V alloy material properties. The PLIF cage was implanted into the intervertebral disc space and had material properties of Ti6AI4V alloy. The rod clip-on device was modeled with material properties of epoxy and linear elastic material.

3.3.4 Loading and Boundary Conditions

FEA testing was preformed using ABAQUS FE solver. Each L4-L5 lumbar spine model, with the rod clip-on device attached, was simulated under different types of loading and varying magnitudes to identify the stress that the rod clip-on device would experience.

Simulating the model under compressive exclusive loading, each model was tested under compressive axial loading. To constrain the model the inferior endplate of the L5 vertebrae was fixed in all directions. To constrain all the parts in the model a tie constraint was applied between the interfaces of the screw shafts and bone interface, screw washer and screw shaft, screw tulip and screw washer, screw tulip and posterior rod, as well as the posterior rod and the device. Additionally, for the Model with a PLIF cage, the PLIF cage was tie constrained to the L4-L5 disc space. Compressive loads were applied via connector elements to the superior endplate of the L4 vertebrae. The model was simulated at 500 N, 750 N, 1000 N, 1250 N, 1500 N, 1750 N, 2000 N, and 2250 N. The maximum stresses experience by the rod clip-on device were recorded. The stress experienced by the rod clip-on device wass analyzed at the location of the PZT stack, cross section.

Simulating the model under bending loading, each model was tested under various moment bending loads and different preloads. Similar, the compressive loading simulations, inferior endplate of the L5 vertebrae was fixed in all direction and all components interfaces are tie constrained as before. A compressive preload of 400 N, 500 N, 800 N, 1000 N, 1250 N and 1500 N was applied via connector elements to simulate bodyweight. A 10 N-m bending moment was applied to the superior endplate of the L4 vertebrae by coupled nodes. The bending moment was tested in different directions to simulate the physiological loading of spinal flexion, extension, left bend, right bend, left rotation and right rotation. The maximum

compressive stress was recorded for each implant component and the rod clip-on device, in the same location as before.

To identify the force that would be experienced by the PZT stack contained in the rod clip-on device, an associated force for each stress recorded was calculated with the following equation. The area used for the calculations is the surface area of a quarter ring PZT specimen that would be placed into the device. It was analyzed that the surface area of the PZT quarter ring was 29.99 mm^2, this value was used for all calculations to identify the forces that the PZT stack would experience.

$$\sigma = \frac{F}{A} \quad => \quad F = \sigma * A$$

$$\sigma - Stress\ (Mpa)$$
$$F - Force\ (N)$$
$$A - Area\ (mm^2)$$

Equation 1: Stress and equivalent force

3.4 Results

3.4.1 Compressive Loading

The resultant compressive stresses experienced by the rod clip-on device and the calculated force are shown in Table 2 for the Model without a PLIF cage and Table 3 for the Model with a PLIF cage. Results from both models followed similar trends, as the compressive load was increased the experienced compressive stress in the rod clip-on device was also increased. For the Model without a PLIF cage the greatest compressive stress experienced by the rod clip-on device was 67.5 Mpa from a compressive axial load of 2250 N, while the least compressive stress was 18.8 Mpa at 500 N. However, for the Model with a PLIF cage the greatest and lowest compressive stress experienced by the rod clip-on device was 31.9 MPa and 8.2 MPa at the same compressive axial loads of 2250 N and 500 N, respectively. Comparing the

results from the Model without a PLIF cage and the Model with a PLIF cage, there is a noticeable decrease in the resultant stresses. When the PLIF cage was implanted into the Model with a PLIF cage, the compressive stress decreased an average of 54% from the results seen in the Model without a PLIF cage across all loads.

Table 2: Maximum compressive stress and respective force experienced by the rod clip-on device at the PZT stack location under compressive loading, in the Model without a PLIF cage

Compressive Axial Load (N)	*Maximum Compressive Stress (Mpa)*	*Force (N)*
500	18.8	564
750	27.5	825
1000	35.4	1062
1250	42.8	1284
1500	49.6	1488
1750	55.9	1676
2000	61.8	1853
2250	67.5	2024

Table 3:Maximum compressive stress and respective force experienced by the rod clip-on device at the PZT stack location under compressive loading, in the Model with a PLIF cage

Compressive Axial Load (N)	*Maximum Compressive Stress (Mpa)*	*Force (N)*
500	8.2	246
750	12.2	366
1000	15.9	477
1250	19.5	585
1500	22.8	684
1750	26.1	783
2000	29.1	873
2250	31.9	957

3.4.2 Physiological Bending

Tables 4 and 5 show the results of the physiological spinal motions applied to the Model without a PLIF cage and the Model with a PLIF cage, respectively. The greatest compressive force experience by the rod clip-on device, in the Model without a PLIF cage, was during right bending followed by right rotation, left rotation, flexion, extension and left bending. On the other hand, the greatest compressive force experienced by the rod clip-on device, in the Model with a

PLIF cage, was during flexion, followed by right bending, left rotation, right rotation, left bending and extension. Similar to the compressive axial loading simulation, the overall compressive forces experienced by the rod clip-on device were greater in the Model without a PLIF cage than the Model with a PLIF cage. With the implementation of the PLIF cage, the rod clip-on device in the Model with a PLIF cage experienced and average 57% decrease of compressive force across all preloads and bending moments.

Table 4: Maximum respective compressive force experienced by the rod clip-on device at the PZT stack location under physiological bending, in the Model without a PLIF cage

	Flexion	**Extension**	**Left Bend**	**Right Bend**	**Left Rotation**	**Right Rotation**
Preload (N)	*Compressive Force (N)*	*Compressive Force (N)*	*Compressive Force (N)*	*Compressive Force (N)*	*Compressive Force (N)*	*Compressive Force (N)*
400	522	381	288	687	636	681
500	615	492	381	765	711	753
800	879	801	648	1038	924	1056
1000	1029	987	819	1209	1095	1083
1250	1212	1203	1017	1407	1293	1272
1500	1413	1479	1203	1595	1505	1473

Table 5: Maximum and respective compressive force experienced by the rod clip-on device at the PZT stack location under physiological bending, in the Model with a PLIF cage

	Flexion	**Extension**	**Left Bend**	**Right Bend**	**Left Rotation**	**Right Rotation**
Preload (N)	*Compressive Force (N)*	*Compressive Force (N)*	*Compressive Force (N)*	*Compressive Force (N)*	*Compressive Force (N)*	*Compressive Force (N)*
400	291	102	168	231	258	225
500	333	147	213	276	288	258
800	453	285	339	405	393	396
1000	525	369	417	483	471	462
1250	612	471	513	576	564	537
1500	693	561	597	663	651	612

3.5 Discussion

The results from the compressive exclusive study show that the rod clip-on device will experience a greater compressive stress at greater loads applied to the lumbar spine. This was consistent across both FEA model. Since PZT is a piezoelectric material, it requires dynamic loading to be able to produce a constant electrical output. This is best compared to walking,

every step that a patient takes puts an increased compressive force on the lumbar spine. Cromwell et al. calculated that the internal forces acting on the lumbar trunk result in an experienced peak spine compression of 1.2 times bodyweight during walking. Cappozzo et al. discovered the external forces acting on the trunk can result in 1.45 times bodyweight during walking. With these findings Rohlmann et al. investigated the loads on posterior instrumentation during walking and notice that each rod experienced a greater maximum force when a step was made with the ipsilateral leg. [25-27] During a normal gait cycle, there are two peaks in the forces experience by the lumbar spine during each step. First is during the heal strike (heal of the foot strikes the ground), and the next is during the push off (toe of the foot pushes off the ground) seen in Figure 12. Where push off produces a greater maximum force out of the two.

For this study, 1.5 times bodyweight was used to identify the stresses experienced on the rod clip-on device. The compressive loading simulated in this study investigates a variety of forces experience at 0.4 - 1.8 times bodyweight, 1250 N. At 1.5 times simulated bodyweight, 1875 N compressive force would be applied to the lumbar spine. Since FEA performed in this study was observed static loading, the maximum compressive stress the rod clip-on device experiences during walking can be discovered by interpolating the results at 1875 N. The Model without a PLIF cage results in a compressive stress of 58.9 Mpa and the Model with a PLIF cage results in a compressive stress of 27.9 Mpa. PZT being a dynamic material, it will produce an electric potential proportional to the increase in stress that is applied to it. While under static loading, nothing will occur. Hence, the difference in stress between bodyweight and 1875 N was analyzed. At bodyweight the PZT stack contained in the rod clip-on device experiences a constant load. With the device implanted on the right posterior rod, as the subject takes a step with the right leg, an 1875 N compressive force is applied to the lumbar spine during push off.

The rod clip-on device experiences an increase in stress of 16.1 MPa and 8.4 MPa in the Model without a PLIF cage and the Model with a PLIF cage, respectively. With the increase in stress the PZT stack produces a proportional electrical potential that can be used for electrical stimulation of the fusion site.

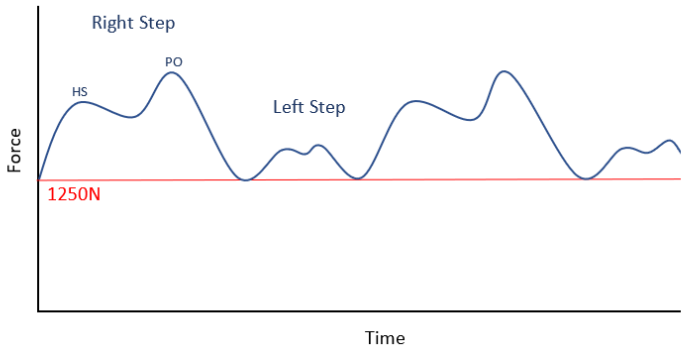

Figure 13: Schematic plot of forces experienced by device attached to right posterior rod during walking. Adapted from Ref. [22]

The results from the physiological bending simulations show that the rod clip-on device can experience a compressive stress during different spinal movements. For a subject implanted only with pedicle screws and posterior rods, like in the Model without a PLIF cage, right bending would produce a maximum compressive force on the PZT stack contained in the rod clip-on device. Meanwhile, a subject also implanted with the same rods and screws along with a PLIF cage, like in the Model with a PLIF cage, flexion would produce a maximum compressive force.

Most of the time pedicle screws and posterior rods are accompanied by an interbody cage for spinal fusion operations to enhance the stability of the fusion site. [30, 31] Even if the interbody disc pace isn't implanted with a device, it will most likely be packed with bone graft to help with the bone remodeling process. Because of this less force will act on the posterior rods and thus the device would also experience less force. Even through the rod clip-on device

experiences a 54% and 57% decrease in the compressive and bending simulations, when a PLIF cage was implanted, these results offer the most realistic values to clinical practice.

3.6 Conclusion

This study shows that a clip-on device implemented on to a posterior rod experienced stress during physiological loading in FEA simulated compressive and bending scenarios. The stress experienced by the device could be used to identify the compressive stress and forces actin on a PZT stack contained in the rod clip-on device. With the PZT stack experiencing a dynamic load, an eclectic potential is created and can be used for theoretical electrical stimulation applied to the fusion site.

3.8 References

1. "Fracture - Mediniche, Inc." [Online]. Available: https://www.mediniche.com/fracture.html. [Accessed: 15-Nov-2020].
2. "Arm Injury Statistics | Aids for One Armed Tasks" [Online]. Available: https://u.osu.edu/productdesigngroup3/sample-page/. [Accessed: 15-Nov-2020].
3. Kalfas, I. H., 2001, "Principles of Bone Healing," Neurosurgical Focus, **10**(4), pp. 1–4.
4. Daniell, J. R., and Osti, O. L., 2018, "Failed Back Surgery Syndrome: A Review Article," Asian Spine J, **12**(2), pp. 372–379.
5. Sandén, B., Försth, P., and Michaëlsson, K., 2011, "Smokers Show Less Improvement than Nonsmokers Two Years after Surgery for Lumbar Spinal Stenosis: A Study of 4555 Patients from the Swedish Spine Register," Spine, **36**(13), pp. 1059–1064.
6. Jackson, K. L., and Devine, J. G., 2016, "The Effects of Obesity on Spine Surgery: A Systematic Review of the Literature," Global Spine J, **6**(4), pp. 394–400.
7. Yasuda, I., *Piezoelectricity of Living Bone.* Journal of Kyoto Prefectural University of Medicine, 1953. **53**(325).
8. Fukada, E. and I. Yasuda, *On the Piezoelectric Effect of Bone.* Journal of the Physical Society of Japan, 1957. **12**(10): p. 5.
9. Lavine, L. S., and Grodzinsky, A. J., 1987, "Electrical Stimulation of Repair of Bone.," JBJS, **69**(4), pp. 626–630.
10. Black, J., 1986, "Electrical Stimulation: Its Role in Growth, Repair and Remodeling of the Musculoskeletal System."
11. Griffin, M., and Bayat, A., 2011, "Electrical Stimulation in Bone Healing: Critical Analysis by Evaluating Levels of Evidence," Eplasty, **11**.
12. Anton, S. R., and Sodano, H. A., 2007, "A Review of Power Harvesting Using Piezoelectric Materials (2003–2006)," Smart Mater. Struct., **16**(3), p. R1.
13. Guerin, S., Tofail, S. A. M., and Thompson, D., 2019, "Organic Piezoelectric Materials: Milestones and Potential," NPG Asia Materials, **11**(1), pp. 1–5.

14. Friis, E.A., S.N. Galvis, and P.M. Arnold, *DC Stimulation for Spinal Fusion with a Piezoelectric Composite Material Interbody Implant: An Ovine Pilot Study*. 2015.
15. Goetzinger, N.C., et al., *Composite piezoelectric spinal fusion implant: Effects of stacked generators.* J Biomed Mater Res B Appl Biomater, 2016. **104**(1): p. 158-64.
16. Krech, E.D., et al., *Effect of compliant layers within piezoelectric composites on power generation providing electrical stimulation in low frequency applications.* J Mech Behav Biomed Mater, 2018. **88**: p. 340-345.
17. Cunningham, C., 2020, "Design and Testing of a Piezoelectric Intramedullary Nail," M.S., University of Kansas
18. Mm, P., Tr, O., I, Y., and Jj, C., 1994, "Mechanical Behavior of the Human Lumbar and Lumbosacral Spine as Shown by Three-Dimensional Load-Displacement Curves.," J Bone Joint Surg Am, **76**(3), pp. 413–424.
19. Goel, V. K., Lim, T.-H., Gwon, J., Chen, J.-Y., Winterbottom, J. M., Park, J. B., Weinstein, J. N., and Ahn, J.-Y., 1991, "Effects of Rigidity of an Internal Fixation Device A Comprehensive Biomechanical Investigation:," Spine, **16**(Supplement), pp. S155–S161.
20. Goel, V. K., Monroe, B. T., Gilbertson, L. G., and Brinckmann, P., 1995, "Interlaminar Shear Stresses and Laminae Separation in a Disc: Finite Element Analysis of the L3-L4 Motion Segment Subjected to Axial Compressive Loads," Spine, **20**(6), pp. 689–698.
21. Goel, V. K., Grauer, J. N., Patel, T. C., Biyani, A., Sairyo, K., Vishnubhotla, S., Matyas, A., Cowgill, I., Shaw, M., Long, R., Dick, D., Panjabi, M. M., and Serhan, H., 2005, "Effects of Charité Artificial Disc on the Implanted and Adjacent Spinal Segments Mechanics Using a Hybrid Testing Protocol," Spine, **30**(24), pp. 2755–2764.
22. Sairyo, K., Masuda, A., Vishnubhotla, S., Faizan, A., Biyani, A., Ebraheim, N., Yonekura, D., Murakami, R.-I., and Terai, T., 2006, "Three-Dimensional Finite Element Analysis of the Pediatric Lumbar Spine. Part I: Pathomechanism of Apophyseal Bony Ring Fracture," European spine journal : official publication of the European Spine Society, the European Spinal Deformity Society, and the European Section of the Cervical Spine Research Society, **15**, pp. 923–9.
23. Sairyo, K., Goel, V. K., Vadapalli, S., Vishnubhotla, S. L., Biyani, A., Ebraheim, N., Terai, T., and Sakai, T., 2006, "Biomechanical Comparison of Lumbar Spine with or without Spina Bifida Occulta. A Finite Element Analysis," Spinal Cord, **44**(7), pp. 440–444.
24. Sairyo, K., Goel, V. K., Biyani, A., Ebraheim, N., Masuda, A., and Liu, J., 2005, "Decompression Surgery For Lumbar Spondylolysis Without Fusion: A Review Article," The Internet Journal of Spine Surgery, **2**(2).
25. Cappozzo, A., 1983, "The Forces and Couples in the Human Trunk during Level Walking," Journal of Biomechanics, **16**(4), pp. 265–277.
26. Cappozzo, A., 1983, "Compressive Loads in the Lumbar Vertebral Column during Normal Level Walking," Journal of Orthopaedic Research, **1**(3), pp. 292–301.
27. Cromwell, R., Schultz, A. B., Beck, R., and Warwick, D., 1989, "Loads on the Lumbar Trunk during Level Walking," Journal of Orthopaedic Research, **7**(3), pp. 371–377.
28. Rohlmann, A., Arntz, U., Graichen, F., and Bergmann, G., 2001, "Loads on an Internal Spinal Fixation Device during Sitting," Journal of Biomechanics, **34**(8), pp. 989–993.
29. 1997, "Loads on an Internal Spinal Fixation Device during Walking," Journal of Biomechanics, **30**(1), pp. 41–47.

30. Bozkus, H., Chamberlain, R. H., Perez Garza, L. E., Crawford, N. R., and Dickman, C. A., 2004, "Biomechanical Comparison of Anterolateral Plate, Lateral Plate, and Pedicle Screws-Rods for Enhancing Anterolateral Lumbar Interbody Cage Stabilization," Spine, **29**(6), pp. 635–641.
31. Cagli, S., Crawford, N. R., Sonntag, V. K., and Dickman, C. A., 2001, "Biomechanics of Grade I Degenerative Lumbar Spondylolisthesis. Part 2: Treatment with Threaded Interbody Cages/Dowels and Pedicle Screws," J Neurosurg, **94**(1 Suppl), pp. 51–60.

Chapter 4: Conclusions and Future Work

4.1 Conclusion

The goal of this study was to identify the stress transferred to a clip-on device attached to a posterior rod for lumbar fixation in FEA. It was concluded that FEA lumbar spine model that incorporates a PLIF cage, provided the most relevant results to clinical practice as most L4-L5 spinal fusions incorporate interbody cages or fill in the intervertebral disc space with bone graft. The rod clip-on device experienced very little compressive stress and thus would induce a low compressive load on the PZT stack. Even through the PZT stack was placed in the anterior position of the rod clip-on device, is does maximize the compressive loading, yet this limits the amount of PZT material that can be used due to the lack of space.

The current work of Downing et al. investigates the power generation of a single PZT ring. [Unpublished] Using the current findings of Downing et al. shows that the PZT stack under these low compressive loads would result in very little electrical output in single layer fusion applications, especially an L4-L5 fusion. If the device is incorporated into an L1-L2 spinal fusion, the larger compressive forces shown in the Model without a PLIF cage can be taken into consideration where the L1-L2 disc space is sometimes left alone. Thus, it is concluded that in L4-L5 practical application the PZT stack contained in the rod clip-on device may not experience a great enough load for the electric properties to be used in beneficial electrical stimulation, but the potential use of incorporating the device onto other posterior rod configurations shows promise.

4.2 Limitations

There are several limitations with this study. The FEA simulations in this study observed static loading to the lumbar spine, piezoelectric material is a dynamic material and is usually

studied under cyclic loading. Testing the rod clip-on device under cyclic loading would provide more accurate results. Device design was simplified for the FEA models. The FEA design removed the spot for the set screw and filled it in with solid material. This was done to create a better constraint between the device and the posterior rod. The study does not identify the results of the forces place on by tightening the set screw on to the rod. Also, it does not identify what would happen if the set screw would become loose during the healing process. Lastly, piezoelectric material such as PZT was not directly tested in the rod clip-on device nor was it simulated in the FEA model. It cannot be directly said if the rod clip-on device is able to produce enough of a direct current signal to be beneficial for electrical stimulation. Comparisons can be made based on previous work done by Cunningham et al. with his PZT ring stack study and current studies being performed by Downing et al. with his single PZT ring study and quarter ring PZT stack study.

4.3 Future work

Future work for this study should investigate cyclic loading, physiological walking, of the lumbar spine with the device implemented on a posterior rod, with a PLIF cage implanted into the intervertebral disc space. This would provide results closest to clinal practice.

Implementation of piezoelectric material specimen into the rod clip-on device would provide a better understanding of the potential power output. This device has very limited space for a PZT stack to be implemented. Using the findings from Goetzinger et al. and Krech et al. a PZT stack could be made to optimize the stresses experienced in posterior fixation.

This study only investigated the application of an L4-L5 lumbar fusion. Further studies should analyze the compressive forces on the rod clip-on device implanted onto a variety pedicle screws and posterior rod configurations such as a T10-Pelvis or a T4-Pelvis system. With the

posterior rod spanning a larger segment of the spine, multiple devices could be used to take advantage of the compressive forces across the instrumentation.

It has been shown that ultrasound can be used to stimulate piezoelectric material. Immediately after spinal fixation surgery the patient will be on bed rest for a period. During that iteration the rod clip-on device will not be able to be stimulated through compressive loading. It was identified that stimulating the PZT stack parallel to is poling direction could result in power generation. A new design concept was developed to adapt to these parameters. Since biomechanical compression was no longer needed, the PZT stack could be placed on the lateral side of the device, where surgeons recommend placing the bulk of the device in the first place. The orientation of the stack was rotated to be stacked and placed anterior to posterior. The space limitations have increased so a larger stack, with CLACS would be able to be used in this device.

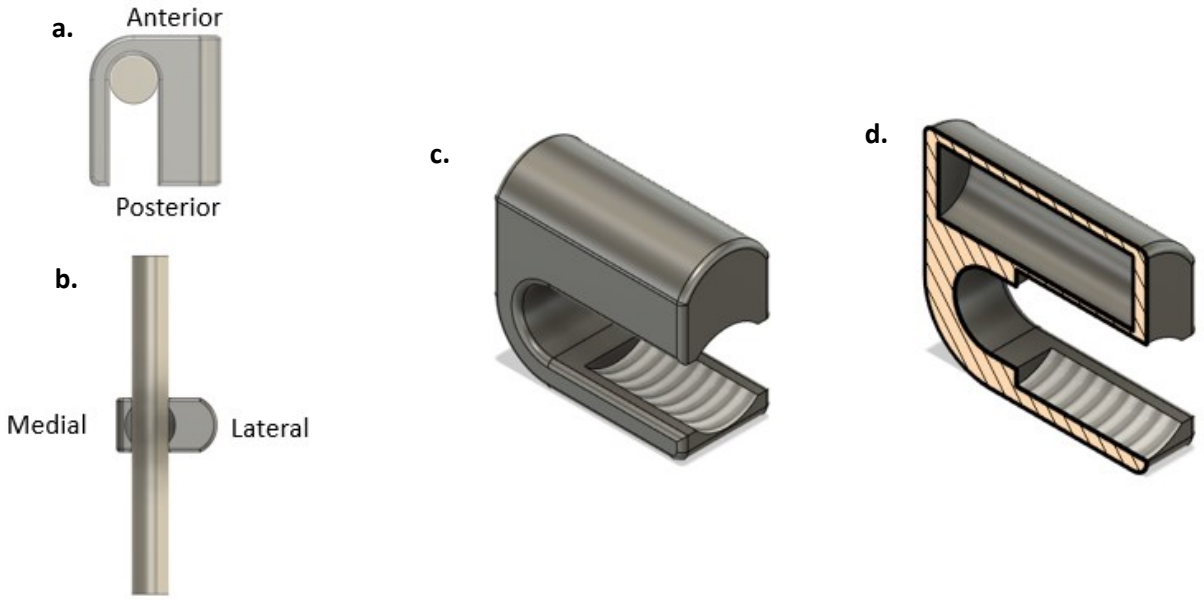

Figure 14: ultrasound device design a) Top view of device on posterior rod, b) Posterior view of device on posterior rod, c) Isometric view of device and d) Cross sectional isometric view of device

Appendix A: Detailed Methods

3D Printed Prototype Fabrication

a. Design part in CAD program (SolidWorks and Fusion 360)
b. Export files as STL
c. Upload STL files to Ultimaker Cura to be sliced and converted into G-Code
d. Upload G-Code to 3d printer
e. Fabricate parts on an Ender 3 Pro material extruder printer equipped with a 0.4 mm extruder nozzle ($\pm$ 0.1 mm resolution) and a print bed of 220 mm x 220 mmx 250 mm. Print Nozzle: 205 C^o and Print Bed 60 C^o.

Silicon Mold Fabrication

a. Manufacture 3D printed prototype
b. Hot glue 4 pieces of small plexiglass together to create a box on a piece of delron, to make a container for silicon mold
c. Tape 3D printed prototype on to the piece of delron, inside the plexiglass box, to make sure 3D printed prototype does not float to the top of the silicon
d. Make approximately 10 g of silicon with a 1:1 ration of Part A and Part B
e. Slowly pour silicon into container with taped down 3D printed prototype
f. Let silicon cure for 2 hours
g. Remove silicon containing the 3D printed prototype out of the container
h. Slowly remove the 3D printed prototype from silicon mold

Epoxy Specimen Fabrication

a. In a plastic cup, carefully measure out 4 g of Part A and 1 g of Part B, of two-part epoxy
b. Slowly mix the two parts, Part A and Part B, together approximately one revolution per second for one minute. Be careful not to stir too quick, this might introduce bubbles into the mix
c. Slowly pour the epoxy mix into the silicon mold
d. Let the epoxy cure for 24 hours
e. Remove epoxy specimen from silicon mold
f. Place epoxy specimen into oven at 65 C^o for 2 hours
g. Let the epoxy specimen cool for 15 min

Appendix B: Other Stress Analysis

Table A: Von-Mises stress experienced by the rod clip-on device at the PZT stack location under physiological bending, in the Model without a PLIF cage

	Flexion	Extension	Left Bend	Right Bend	Left Rotation	Right Rotation
Preload (N)	*Maximum Von-Mises Stress (Mpa)*	*Maximum Von-Mises Stress (Mpa)*	*Maximum Von-Mises Stress (Mpa)*	*Maximum Von-Mises Stress (Mpa)*	*Maximum Von-Mises Stress (Mpa)*	*Maximum Von-Mises Stress (Mpa)*
400	48.1	28.3	20.7	61.4	42.4	49.9
500	55.4	37.3	26.9	69.2	49.5	57.4
800	75.4	61.7	48.9	91.1	71.5	77.4
1000	88.5	76.5	62.5	104.4	85.1	91.9
1250	103.2	93.8	78.3	120.1	100.9	107.4
1500	123.2	110.5	91.3	138.4	116.4	127.4

Table B: Von-Mises stress experienced by the rod clip-on device at the PZT stack location under physiological bending, in the Model with a PLIF cage

	Flexion	Extension	Left Bend	Right Bend	Left Rotation	Right Rotation
Preload (N)	*Maximum Von-Mises Stress (Mpa)*	*Maximum Von-Mises Stress (Mpa)*	*Maximum Von-Mises Stress (Mpa)*	*Maximum Von-Mises Stress (Mpa)*	*Maximum Von-Mises Stress (Mpa)*	*Maximum Von-Mises Stress (Mpa)*
400	46.5	19.3	26.2	44.4	33.7	33.2
500	53.6	27.7	32.1	58.6	41.5	40.9
800	74.1	51.2	54.5	73.8	63.35	62.9
1000	86.8	65.8	67.4	87.5	76.9	76.6
1250	101.9	82.9	82.6	103.7	93.1	92.7
1500	116.2	99.1	97.3	118.8	108.1	107.8

Table C: Maximum compressive stress experienced by the rod clip-on device at the PZT stack location under physiological bending, in the Model without a PLIF cage

	Flexion	Extension	Left Bend	Right Bend	Left Rotation	Right Rotation
Preload (N)	*Maximum Compressive Stress (Mpa)*	*Maximum Compressive Stress (Mpa)*	*Maximum Compressive Stress (Mpa)*	*Maximum Compressive Stress (Mpa)*	*Maximum Compressive Stress (Mpa)*	*Maximum Compressive Stress (Mpa)*
400	17.4	12.7	9.6	22.9	21.2	22.7
500	20.5	16.4	12.7	25.5	23.7	25.1
800	29.3	26.7	21.6	34.6	30.8	35.2
1000	34.3	32.9	27.3	40.3	36.5	36.1
1250	40.4	40.1	33.9	46.9	43.1	42.4
1500	47.1	49.3	40.1	53.2	50.2	49.1

Table D: Maximum compressive stress experienced by the rod clip-on device at the PZT stack location under physiological bending, in the Model with a PLIF cage

	Flexion	Extension	Left Bend	Right Bend	Left Rotation	Right Rotation
Preload (N)	*Maximum Compressive Stress (Mpa)*	*Maximum Compressive Stress (Mpa)*	*Maximum Compressive Stress (Mpa)*	*Maximum Compressive Stress (Mpa)*	*Maximum Compressive Stress (Mpa)*	*Maximum Compressive Stress (Mpa)*
400	9.7	3.4	5.6	7.7	8.6	7.5
500	11.1	4.9	7.1	9.2	9.6	8.6
800	15.1	9.5	11.3	13.5	13.1	13.2
1000	17.5	12.3	13.9	16.1	15.7	15.4
1250	20.4	15.7	17.1	19.2	18.8	17.9
1500	23.1	18.7	19.9	22.1	21.7	20.4

Table E: Maximum tensile stress experienced by the rod clip-on device at the PZT stack location under physiological bending, in the Model without a PLIF cage

	Flexion	Extension	Left Bend	Right Bend	Left Rotation	Right Rotation
Preload (N)	*Maximum Tensile Stress (Mpa)*	*Maximum Tensile Stress (Mpa)*	*Maximum Tensile Stress (Mpa)*	*Maximum Tensile Stress (Mpa)*	*Maximum Tensile Stress (Mpa)*	*Maximum Tensile Stress (Mpa)*
400	17.9	8.6	10.9	21.4	21.7	24.4
500	20.4	11.7	13.5	24.3	24.2	27.1
800	27.5	20.1	20.7	31.9	31.3	36.2
1000	31.9	25.1	25.2	36.7	35.6	38.9
1250	37.1	30.9	30.3	42.3	40.6	44.2
1500	43.5	35.9	35.6	48.7	45.5	49.5

Table F: Maximum tensile stress experienced by the rod clip-on device at the PZT stack location under physiological bending, in the Model with a PLIF cage

	Flexion	Extension	Left Bend	Right Bend	Left Rotation	Right Rotation
Preload (N)	*Maximum Tensile Stress (Mpa)*	*Maximum Tensile Stress (Mpa)*	*Maximum Tensile Stress (Mpa)*	*Maximum Tensile Stress (Mpa)*	*Maximum Tensile Stress (Mpa)*	*Maximum Tensile Stress (Mpa)*
400	8.5	3.7	4.9	7.6	8.5	6.9
500	9.7	5.2	6.2	9.8	9.8	7.9
800	13.2	9.3	9.8	12.9	13.5	11.2
1000	15.4	11.9	12.2	15.3	15.8	13.2
1250	17.8	14.9	14.8	18.1	18.5	15.9
1500	20.2	17.7	17.4	20.8	21.1	18.6

Appendix C: Rod Clip-on Device Electrode Location

Electrode design and location for the rod clip-on device

a. Wires coming out from the device (Figure a.)
    a. This will allow the surgeon to place the electrodes directly where they want to apply the electrical stimulation
b. Face or edge of the device acting as the electrode (Figure b.)
    a. This will simplify the design and apply electrical stimulation to the bone graft directly place around the device

Figure a.

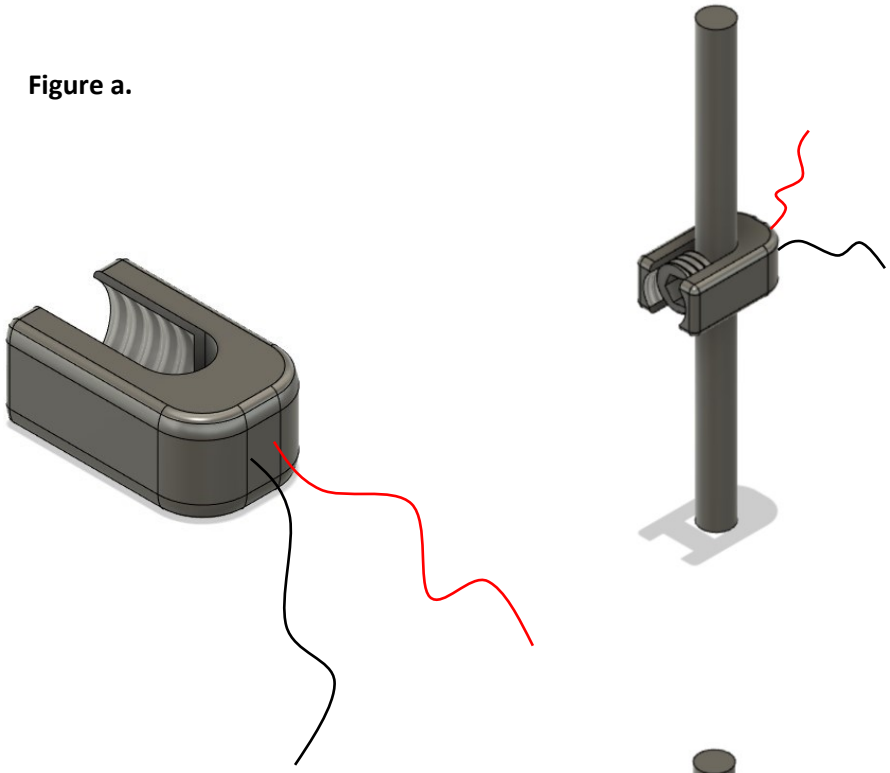

Figure b.